
Conformational and Electronic Study of *N*-Phenylalkyl-3,4-Dichloromaleimides: Ab Initio and DFT Study

MIGUEL A. ZAMORA,¹ MARCELO F. MASMAN,¹
JOSÉ A. BOMBASARO,¹ MÓNICA L. FREILE,²
VALDIR CECHINEL FILHO,³ SILVIA N. LÓPEZ,⁴
SUSANA A. ZACCHINO,¹ RICARDO D. ENRIZ¹

¹*Departamento de Química, Facultad de Química, Bioquímica y Farmacia, Universidad Nacional de San Luis, Chacabuco 917, 5700 San Luis, Argentina*

²*Departamento de Química, Facultad de Ciencias Naturales U.N.P.S.J.B. km 4. 9000, Comodoro Rivadavia, Chubut, Argentina*

³*Núcleo de Investigações Químico-Farmacêuticas, (NIQFAR)/CCS, Universidade do Vale do Itajaí (UNIVALI), Itajaí, SC, Brasil*

⁴*Farmacognosia, Facultad de Ciencias Bioquímicas y Farmacéuticas, Universidad Nacional de Rosario, Sulpacha 531, (2000) Rosario, Argentina*

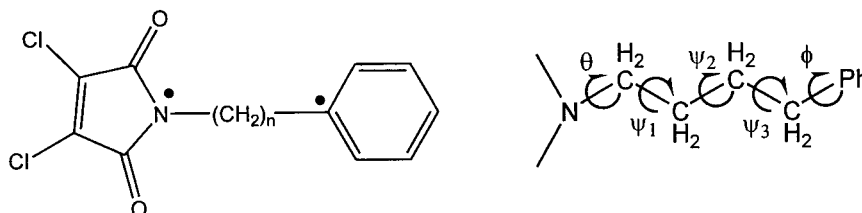
Received 5 June 2002; accepted 30 October 2002

DOI 10.1002/qua.10524

ABSTRACT: A conformational and electronic study on *N*-phenylalkyl-3,4-dichloromaleimides, a new series of antifungal compounds, was carried out. In this study ab initio [RHF/3-21G and RHF/6-31G(*d*)] and density functional theory (B3LYP/6-31G(*d*)) calculations were performed. The effect of solvent (water) was taken into account by performing calculations with the isodensity polarizable continuum model method. The electronic study of the compounds was carried out using molecular electrostatic potentials. The presence of two symmetrical aromatic systems reduces notably the conformational possibilities of these maleimides. The results permit the recognition of the minimal structural requirements for the production of the antifungal response; a 3,4-dichloroimido ring and a benzene ring appear to be indispensable. Also, theoretical calculations suggest that the optimum interatomic distance between these moieties is about 3.5–5.0 Å. © 2003 Wiley Periodicals, Inc. *Int J Quantum Chem* 93: 32–46, 2003

Key words: maleimides; ab initio and DFT calculations; conformational study; antifungal activity

Correspondence to: R. D. Enriz; e-mail: denriz@unsl.edu.ar

TABLE I
General structural feature of maleimides and minimal inhibitory concentration (MIC) values obtained against a panel of human pathogenic fungi.


Compound	<i>n</i>	MIC ($\mu\text{g/mL}$)				
		C.a. ^a	Cr.n. ^b	A.n. ^c	A.fl. ^d	A.fu. ^e
I	0	50	25	50	25	50
II	1	25	12.5	>50	>50	25
III	2	>50	>50	6.25	6.25	6.25
IV	3	6.25	1.56	6.25	6.25	6.25
V	4	25	6.25	25	12.5	25
Amphotericin B		0.75	0.40	0.90	3	3
Ketoconazole		8	2	12.5	30	20

The MIC values were reported in Ref. [8].

^a *Candida albicans* ATCC 10231.

^b *Cryptococcus neoformans* ATCC 32264.

^c *Aspergillus niger* ATCC 9029.

^d *Aspergillus flavus* ATCC 9170.

^e *Aspergillus fumigatus* ATCC 26934.

Introduction

There appears to be a large and impressive array of drugs for the treatment of fungal infections. Unfortunately, the reality is different. There are, in fact, only limited therapeutic options, especially for systemic mycotic infections [1, 2]. Amphotericin B, developed in 1957–1958, remains a widely used antifungal drug, most recently gaining renewed life through lipid-based formulations [3]. In fact, currently available antifungal therapy is less than optimal. It is clear that newer agents are needed to treat the increasing incidence and severity of fungal disease.

As a part of our program aimed at identifying novel antifungal agents, we focused on developing antifungal compounds that would selectively inhibit the synthesis of the fungal cell wall [4–7]. Recently, a series of maleimides was synthesized and assayed for antifungal activity [8]. Concerning the antifungal activity of maleimides, 3,4-dichloromaleimides showed the broadest spectrum of action inhibiting all the fungi tested. Among all derivatives tested, compounds **III–V** displayed the most relevant antifungal effects, compound **IV** be-

ing the most active molecule in this series (denoted in bold in Table I).

Alkyl spacers of different lengths separate the aromatic rings in these homologs. Our previous results [8] suggest that the variation of the alkyl chain length in these maleimides has a drastic effect on the antifungal activity of these compounds. The 3,4-dichloromaleimide homologs with an alkyl chain shortened to one methylene group or without methylene (compounds **II** and **I**, Table I) displayed a weak antifungal activity in comparison with **IV**. The propylene chain of maleimides (compound **IV**) is clearly optimal for the antifungal effect in this series. Elongation of the alkyl chain results in a sudden decrease in potency. Thus, compound **V** displays a lower antifungal activity with respect to **IV**. It is clear that the conformational aspect of each molecule under investigation is a relevant factor, which will give some new insights in the mechanism of action of these compounds at the molecular level. Thus, the alkyl chain methylated maleimide analogs become valuable tools in molecular modeling studies.

The postulate that a molecule has to assume a particular conformation to function at a receptor

implies that the ability of a molecule to achieve the required conformation would affect its activity. This is usually interpreted in the sense that activity will be impaired unless a molecule can assume the active form.

The suggestion that a preferred conformation is the active form carries with it the connotation that the concentration of drug required for an effect could be related to the population of drug molecules in the requisite conformation or, for molecules that are conformationally mobile, to the likelihood of achieving it (depending on the kinetics of conformer interconversion). However, to relate the biologic activity of a ligand to its conformational properties poses considerable problems because it is difficult to devise molecules of a given conformation without changing some other physicochemical properties as well. One approach to this problem might be provided by the use of conformationally mobile analogs where the conformational preferences differ from those of the title compound. We considered, as a corollary to our proposal, that *if minimum energy conformations of 3,4-dichloromaleimides are significant, then an altered conformational preference should be accompanied by a corresponding change in antifungal activity*. Such a relationship would also serve to identify which conformation(s) should be associated with antifungal activity.

In principle, the molecules of interest are flexible compounds, which can adopt a variety of conformations dynamically interconverted one another. Which conformations are of biologic importance is not self-evident and, because they are in equilibrium, the process of interconversion between conformers may have biologic significance. Then, it is imperative to define its 3-D geometry exactly in terms of biologically relevant conformation. By relevant conformation we mean the 3-D arrangement of atoms, which has the adequate shape to produce the biologic response. Active conformations may not be stable in the solid phase or in solution. Indeed, it may not be stable at all except in the receptor environment. Because calculations are equally valid for unstable as well as stable shapes, they answer the following question: Is there a particular conformation of maleimides essential for the antifungal effect? In this work an exhaustive conformational and electronic study of 3,4-dichloromaleimides was carried out using theoretical calculations.

Method of Calculation

To determine the minima on the conformational potential energy surfaces (PESs) of 3,4-dichloromaleimides, fully relaxed ab initio [RHF/3-21G and RHF/6-31G(*d*)] calculations were performed. Correlation effects were included using density functional theory (DFT) with the Becke3–Lee–Yang–Parr (B3LYP) [9] functional and the 6-31G(*d*) basis set.

An extensive search for low energy conformations on the PESs for compounds **IV** and **V** was carried out by using a systematic search routine in connection with the MM2 force field [10]. At first, a systematic conformational search using the GAS-COS algorithm [11–14] developed by our group was carried out. Subsequently, several distinct trial atomic spatial arrangements were used in the geometry optimization jobs using ab initio and DFT methods to locate the possible equilibrium structures present on the multidimensional energy surfaces. Minima were characterized through harmonic frequency analysis employing 3-21G, 6-31G(*d*) basis set and B3LYP/6-31G(*d*) calculations.

The effect of the solvent (water) was calculated by the isodensity polarizable continuum model (IPCM) method [15]. IPCM is more advanced than the polarizable continuum model (PCM) method [16] because in IPCM the cavity of a solute is defined by the electron isodensity surface while in PCM it is defined by the van der Waals surface. The efficiency of this method has been widely recognized in chemical behaviors in solution for small polar molecules [17–20]. It should be emphasized, however, that the evaluation of the solvent effect implies a comparison to the gas-phase results. Thus, both sets of results with and without the solvent are required.

Rotational energy profiles around torsional angles have been determined using RHF/3-21G, B3LYP/6-31G(*d*), and IPCM calculations [B3LYP/6-31++G(*d,p*)/6-31G(*d*)]. The energy has been calculated at 30° intervals of the dihedral angles.

All gas-phase and aqueous-phase calculations were performed using Gaussian 98 [21].

The electronic study of the compounds was carried out by using molecular electrostatic potentials (MEPs). MEPs have been shown to provide reliable information, both on the interaction sites of molecules with point charges and on the comparative reactivities of these sites [22–25]. These MEPs were

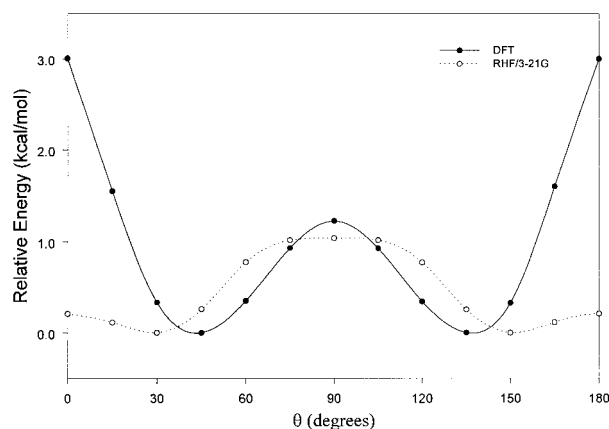


FIGURE 1. Rotational energy barrier profiles computed at the RHF/3-21G and DFT levels of theory obtained for compound **I**.

calculated using RHF/6-31+G(*d*) wave function from the SPARTAN program [26]. DFT/6-31G(*d*)-optimized coordinates were imported into PC SPARTAN. To generate the wave functions, HF/6-31+G(*d*) single-point calculations were performed from PC SPARTAN.

Results and Discussion

CONFORMATIONAL ANALYSIS

The 3,4-dichloroimido ring of 3,4-dichloromaleimides is a planar and rigid regular pentagon; similarly, the benzene ring is a planar regular hexagon. But, maleimides are flexible molecules and rotation occurs at the single bonds in the alkyl chain. The overall shape of the molecule is determined by the orientation of the 3,4-dichloroimido ring (determined by angle θ), the orientation of the benzene ring (determined by angle ϕ), and the conformation of the alkyl chain (determined by angles ψ_1 to ψ_3 , respectively) (Table I).

Compound **I** ($n = 0$) may be regarded as a trivial case. Although its rotation has a four-fold periodicity (Fig. 1), in which the four low-energy minima are degenerated, there is only one unique minimum (conformation **I** in Table II and Fig. 2). Observing the RHF/3-21G curve shown in Figure 1, it is difficult to determine whether the critical point with $\theta = 90^\circ$ is a shallow local minimum of higher energy or extreme point of higher order, e.g., first-order transition structure. For an unambiguous characterisation of this point, ab initio (RHF/3-21G) and DFT [B3LYP/6-31G(*d*)] harmonic frequency

calculations were performed. Both levels of theory indicate that this critical point corresponds to a first-order transition state exhibiting a single negative eigenvalue of the Hessian matrix.

DFT calculations predict that the rotation of the torsional angle θ is poorly restricted with an energy barrier of 1.1 kcal/mol for the interconversion between the conformers (Fig. 1).

Compound **II** ($n = 1$) looks like a simple conformational problem with two torsional angles (θ and ϕ). The feature of this surface is given in Figure 3. The PES has four minima but they are all equivalent. Thus, compound **II** displays only one conformation (Table II and Fig. 2). These results are in agreement with those previously reported for diphenylmethane [27] and other structurally related molecules [28].

In compound **III** ($n = 2$), when a planar moiety of two-fold symmetry is connected to a tetrahedral carbon of three-fold symmetry, the torsional conformational potential about that single bond does not necessarily have three minima; in principle, it may have six minima, as in the case of methylbenzene [29]. In ethylbenzene [30], however, the six degenerated minima are reduced to two unique structures.

In compound **III** the orientations of the ring systems are described by the dihedral angles θ and ϕ , respectively, whereas the orientations of the alkyl chain are described by the dihedral angle ψ_1 . Multidimensional conformational analysis (MDCA) [31–33] predicts the existence of $2 \times 3 \times 2 = 12$ legitimate minima for triple rotors with these multiplicities. However, ab initio and DFT calculations indicate that molecule **III** possesses only two different spatial orderings: folded (**IIIa**) and extended (**IIIb**) (Fig. 2). The extended methylene orientation represents the global minimum at the DFT level; the energy difference between the two low-energy conformations, however, is small, only 0.73 kcal/mol (Table III).

The conformational analysis of compound **III** requires at this point the evaluation of the flexibility, i.e., the energy determination of the transitional barrier between the predicted conformers **IIIa** and **IIIb**. This is of crucial importance because, if the barriers are low, during molecular recognition a molecule could be converted, with a low energy cost, to a preferred geometry in the binding site within the receptor. In Figures 4(a)–4(c) RHF/3-21G and DFT energies are plotted vs. rotation angles θ , ϕ , and ψ_1 for conformation **IIIb**. It should be noted that the energy scales in the figures are not

TABLE II
Torsional angles obtained for the different conformations of compounds I–V, at MM2, ab initio (RHF/3-21G), and DFT [B3LYP/6-31G(d)] levels of theory.

Compound	Conformation	θ (°)		ϕ (°)		ψ_1 (°)		ψ_2 (°)		ψ_3 (°)						
		MM2	Ab initio	DFT	MM2	Ab initio	DFT	MM2	Ab initio	DFT	MM2	Ab initio	DFT			
I	I	11.92	29.14	43.57												
	II	88.85	86.64	87.87	89.43	89.08	89.38									
	III	76.54	57.87	66.27	79.18	75.11	74.15	53.61	56.88							
IV	IIIa	85.31	80.64	88.56	86.37	89.40	89.08	180.36	180.05							
	IIIb	91.01	93.97	88.76	88.53	88.27	88.92	179.81	180.01	181.25	179.98	180.01				
	IVa	66.15	73.99	77.40	59.84	83.25	81.28	71.79	73.76	60.06	74.34	73.66				
	IVb	90.25	104.26	91.28	75.43	72.53	71.20	179.55	176.97	63.45	62.86	62.88				
V	IVc	66.43	64.68	70.08	121.7	121.83	122.10	60.88	65.96	65.11	290.86	286.19	285.60			
	IVd	76.17	69.42	79.59	83.07	85.22	85.87	60.71	60.29	63.17	177.59	176.24	176.73			
	IVe	88.68	102.04	91.12	274.58	271.38	269.56	178.62	178.36	176.85	70.00	69.28	66.07	177.91		
	Va	88.84	89.71	88.63	88.76	88.77	89.07	179.55	180.00	180.00	180.00	180.03	180.00	179.37	179.98	180.00
	Vb	72.34	69.73	80.96	103.86	105.12	104.98	58.85	61.11	62.48	177.00	176.45	176.46	296.22	294.32	294.24
	Vc	104.26	98.10	101.24	265.33	257.42	263.85	297.97	295.14	291.92	88.06	90.48	86.43	182.12	184.58	181.85
	Vd	83.93	74.14	85.23	76.51	74.97	73.34	179.44	179.71	180.29	175.56	178.78	179.56	61.04	64.90	65.07
	Ve	72.37	77.18	80.63	267.11	270.88	270.00	57.82	59.20	62.26	68.79	65.63	66.28	181.00	183.37	181.00
	Vf	105.06	101.34	103.06	257.70	242.35	250.02	291.62	290.09	288.03	267.69	261.11	264.99	61.56	56.18	58.85
	Vg	85.29	75.05	86.91	289.36	279.00	292.29	179.55	186.19	177.38	84.07	85.17	75.73	294.05	286.14	287.46
VI	Vh	74.51	67.63	77.12	88.18	87.57	87.01	59.10	60.36	61.90	177.34	176.47	177.50	178.15	178.65	178.69
	Vi	76.03	73.75	83.67	77.09	76.37	75.67	63.52	63.76	66.29	178.36	178.02	178.15	64.31	66.78	65.99
	Vj	90.37	89.78	93.57	256.37	264.96	264.89	178.62	189.61	186.39	67.68	72.14	71.27	60.21	65.90	65.70
	Vk	110.23	109.87	105.98	232.75	251.19	260.65	285.75	270.47	300.95	78.06	74.14	93.20	53.56	63.00	67.41
	VI	74.10	72.26	78.85	252.11	245.36	248.26	62.03	58.32	61.94	67.45	61.33	64.33	58.86	56.52	60.24
	Vm															
	Vn															

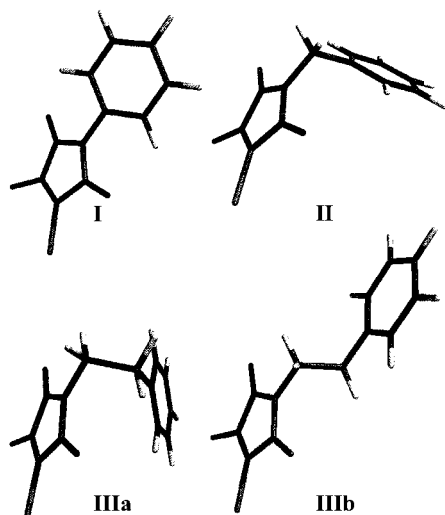


FIGURE 2. Spatial view of the different conformations obtained for compounds **I**, **II**, and **III** (geometries were obtained from DFT calculations).

the same, in an attempt to make the differences as clear as possible. Looking first at the torsional angles θ and ϕ [Figs. 4(a) and 4(b)] we see that the global minimum was found to be the one in which the planar moiety was perpendicular to the C—C bond (θ and $\phi \cong 90^\circ$). Of course, both of these minima occurred twice in full 360° rotation due to the fact that the two sides of the 3,4-dichloroimido and benzene rings are identical. The barriers at $\theta = 0$ and 180° are relatively high, 7.8 kcal/mol at the DFT level, about twice as high as that in ϕ , in which it is 3.6 kcal/mol. The difference in the heights of the θ barriers is due to the strong steric repulsion of the carbonyl groups, which are present in the 3,4-dichloroimido ring. Similar potential energy scans were performed for the torsional angle ψ_1 in the two different conformations **IIIb** and **IIIa** [Figs. 4(c) and 4(d), respectively]. Both figures exhibit two minima: The first is at a dihedral angle of about 60° and the other at the dihedral angle of 180° . The orientation of the CH_2 group at a dihedral 60° angle refers to *gauche* orientation (folded form, **IIIa**) and 180° to *anti* orientation (extended form, **IIIb**). These curves display a relatively shallow low-energy region between the *gauche* and *anti* conformation and a larger *cis* barrier. The rotational barrier at 120° in conformation **IIIb** is relatively low, 4.54 kcal/mol at the DFT level, whereas this barrier is 4.14 kcal/mol for conformation **IIIa**. Thus the gas-phase results indicate a mixture of two conformers with a slight predominance of the extended one.

At this stage of our work we assume that solvent effects could change these results somewhat. To verify this assumption we attempted to add this effect to the computations. For this sake, we adopted the IPCM, which defines the cavity as an isodensity surface of the molecule [15]. We do not expect that the entire solution behavior of 3,4-dichloromaleimides be explained by such a reduced treatment. The aim of these calculations is less ambitious: We intend to obtain a reasonable indication of the direction and magnitude of changes in conformational preferences of the isolated molecule when it enters aqueous solution. From this point of view, the inclusion of the IPCM model in the computations should be in particular significant. DFT/IPCM calculations indicate the folded conformation (**IIIa**) as the preferred form for compound **III**. This is a striking difference from the DFT gas-phase results. The energy gap between the global minimum and the extended conformation (**IIIb**) is 1.34 kcal/mol (Table III). Thus, there is a wider energy difference between the two conformations at the DFT/IPCM level than that obtained in the gas phase. Figures 4(a) and 4(b) show the potential energy curves obtained for torsional angles θ and ϕ from DFT/IPCM calculations. These results are similar to those obtained by using DFT gas-phase computations. Figures 4(c) and 4(d) illustrate the results for the hydrated molecule **III**, indicating a profound change with respect to the results for the isolated molecule depicted in the same figures. For

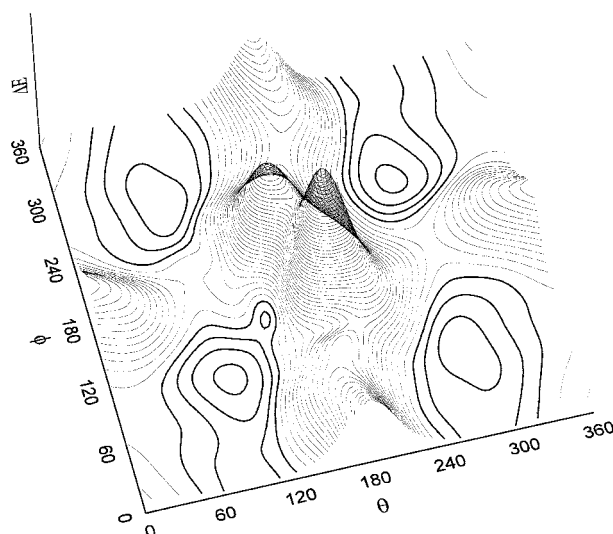


FIGURE 3. Conformational PES obtained for compound **II** from RHF/3-21G calculations. Full cycle of rotation (from 0 – 360°) is shown for variables θ and ϕ .

TABLE III

Relative energies obtained for the different conformations of compounds I–V, at MM2, ab initio [RHF/3-21G and RHF/6-31G(d)], DFT [B3LYP/6-31G(d)], and DFT/IPCM [B3LYP/6-31++G(d,p)//6-31G(d)] levels of theory.

Compound	Conformation	MM2 ΔE (kcal/mol)	Ab initio			DFT/IPCM ΔE (kcal/mol)	Interatomic distance (Å) ^a
			RHF/3- 21G ΔE (kcal/mol)	RHF/6- 31G(d) ΔE (kcal/mol)	DFT ΔE (kcal/mol)		
I	I						1.4
II	II						2.5
III	IIIa	0.00	0.26	0.91	0.73	0.00	3.0
	IIIb	1.11	0.00	0.00	0.00	1.34	3.8
IV	IVa	1.62	1.76	0.00	0.00	0.00	5.0
	IVb	2.12	0.00	0.94	0.22	2.08	4.1
	IVc	1.79	1.78	0.61	0.43	2.84	4.5
	IVd	0.00	1.58	1.22	1.05	4.33	3.2
	IVe	1.64	1.81	0.67	0.42	4.70	4.5
V	Va	1.02	2.36	1.19	0.97	0.00	6.0
	Vb	0.10	1.53	0.00	0.00	2.43	6.4
	Vc	0.50	1.52	1.05	0.66	2.49	5.5
	Vd	1.18	2.42	2.88	2.15	4.05	4.7
	Ve	0.23	1.73	0.68	0.49	5.50	5.5
	Vf	0.55	0.00	0.83	0.16	5.85	5.0
	Vg	2.02	3.06	3.56	2.71	6.43	4.5
	Vh	1.42	2.57	2.45	1.80	6.94	4.7
	Vi	0.00	1.74	0.82	0.58	7.11	5.5
	Vj	0.04	1.92	1.30	0.90	7.50	5.0
	Vk	0.68	0.72	1.29	0.63	Not found ^b	5.0
VI	1.11	4.82	3.82	2.82	Not found ^b	4.4	
Vm	1.04	1.04	1.70	0.93	Not found ^b	4.9	

In the ΔE columns, the global minimum for each compound is denoted in bold. The interatomic distances obtained at the DFT level are also shown.

^a Distance between N*–C* in Table I.

^b Maximum number of iterations exceeded.

conformation **IIIb**, in place of one deep minimum for the *anti* form in Figure 4(c) we now observe *gauche* ($\psi_1 \cong 60^\circ$) and *anti* ($\psi_1 \cong 180^\circ$) minima of almost equal energy at the DFT/IPCM level. In contrast, for conformation **IIIa** [Fig. 4(d)], although the global energy minimum still corresponds to a *gauche* form ($\psi_1 \cong 60^\circ$), it is now limited to narrow values of ψ_1 associated with the folded arrangement of the side-chain with respect to the ring. Moreover, the local energy minimum (extended form) appears now at 2.62 kcal/mol above the global one, suggesting the possible occurrence of such a conformer in equilibrium with the predominant *gauche* one but in a proportion smaller than that expected in the gas phase.

Compound **IV** ($n = 3$) is, in principle, a quadruple rotor and therefore its conformational change is governed by four circular motions involving θ , ϕ ,

ψ_1 , and ψ_2 torsional angles. MDCA predicts the existence of $2 \times 3 \times 3 \times 2 = 36$ legitimate minima for a quadruple rotor with these multiplicities. Using MM2 and RHF/3-21G calculations, in contrast to the idealized topology, only 5 different conformations instead of 36 were found (Table II). DFT and DFT/IPCM calculations confirm only five different conformations for this molecule (conformations **IVa–IVe**, Table II and Fig. 5). To categorize the structures obtained we introduced, intuitively rather than by a precise definition, four forms: fully folded (FF), open folded (OF), open extended (OE), and fully extended (FE). By FF form we understand a closed structure with relatively short distances between the aromatic rings. By FE form we understand a form with linearized connecting chain. By OF we denote a form intermediate between folded and extended. The global minimum varies as a

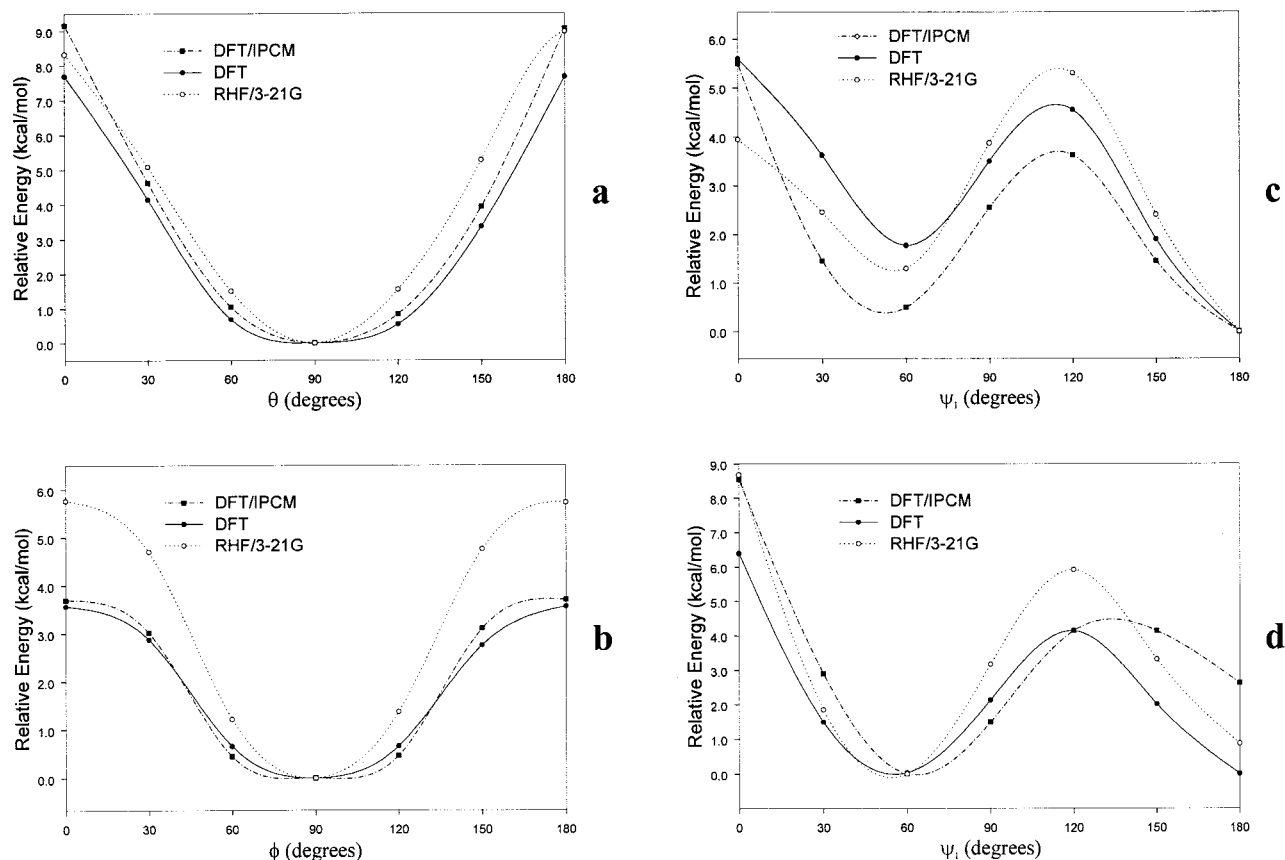


FIGURE 4. Comparison of PECs of torsional angles θ , ϕ , and ψ_1 obtained for compound **III** in the extended conformation (**IIIb**) (a, b, and c). The torsional angle ψ_1 in the folded conformation (**IIIa**) is also shown (d); each PEC was calculated at RHF/3-21G, DFT, and DFT/IPCM levels of theory.

function of the basis set or level of theory: **IVa** at RHF/6-31G(d), DFT, and DFT/IPCM levels, **IVd** at the MM2 level, and **IVb** at the RHF/3-21G level (Table III). However, it can be seen from Table II that there is an overall agreement between the empirical and quantum mechanical calculations regarding the torsion geometric parameters for the global and local minima.

The situation prevalent in solution has been investigated again following the IPCM model. The results obtained for compound **IV** are shown in Table III and Figure 6. It is seen that the conformationally allowed space for hydrated molecule **IV** is substantially reduced with respect to the isolated molecule and that, moreover, although different conformations are still available, on the probability scale there is a definite advantage for the fully extended form, as can be observed from the energy gaps shown in Table III.

Figures 6(a) and 6(b) present the results for the hydrated conformation **IVa** and also in this case

substantial changes are observed compared to the results for the isolated molecule depicted in the same figures. In place of two minima *gauche* (ψ_1 and $\psi_2 \cong 60^\circ$) and *anti* (ψ_1 and $\psi_2 \cong 180^\circ$) of almost the same energy, we observe a deep minimum for the *anti* form. The energy barriers between the *gauche* and *anti* conformers are 5.5 kcal/mol at the DFT/IPCM level and 2.9 kcal/mol at the DFT level, whereas the energy barriers between *gauche* forms are 8.7 and 4.9 kcal/mol, respectively. It is clear that DFT/IPCM calculations predict energy barriers higher than those obtained using DFT (gas-phase) computations. At this stage of our work we consider the trend predicted for the solution effect as certainly significant.

Figures 6(c) and 6(d) show the rotational behavior of the ψ_1 and ψ_2 torsional angles in conformation **IVb**. In this case, both DFT (gas-phase) and DFT/IPCM calculations display closely related results. The energy difference between the minima near 60 and 180° is small, only 0.48 kcal/mol at the DFT

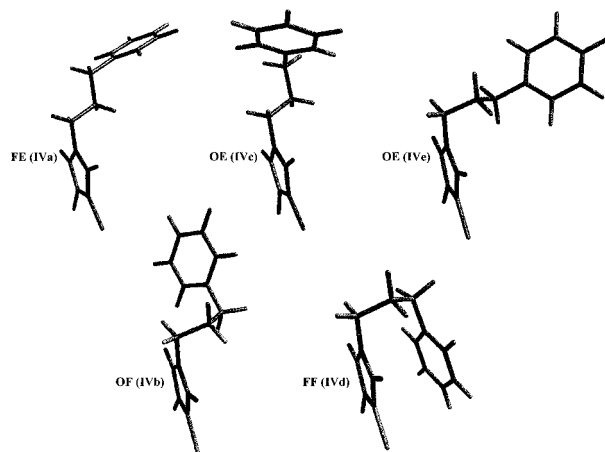


FIGURE 5. Spatial view of the five different conformations obtained for compound **IV** (geometries were obtained from DFT calculations).

level and even less with the DFT/IPCM method [0.006 kcal/mol, Fig. 6(d)]. The rotational barriers at about 120° are low, ≈ 3.5 and 3.0 kcal/mol at the DFT/IPCM and DFT levels, respectively. The *cis* barriers at 0° are larger, ≈ 11.5 and 11.1 kcal/mol. In short, these results may indicate that the structure of **IV** in water is not as flexible as we expected but rather limited, restricted to FE, OE, and OF forms.

Compound **V** ($n = 4$) is a quintuple rotor and therefore its conformational change is governed by five circular motions involving θ , ϕ , ψ_1 , ψ_2 , and ψ_3 torsional angles. MDCA predicts the existence of $2 \times 3 \times 3 \times 3 \times 2 = 108$ legitimate minima for a quintuple rotor with the above multiplicities. However, MM2 and RHF/3-21G calculations indicate the existence of only 13 different conformations (**Va–Vm** in Table II); the rest were annihilated or equivalents. The following types of structures were found:

1. FE structures with the three torsional angles (ψ_1 – ψ_3) in *anti* ($\approx \pm 180^\circ$).
2. OE structures with one torsional angle in *gauche* ($\approx \pm 60^\circ$) and two in *anti*.
3. OF structures with two torsional angles in *gauche* and one in *anti*.
4. FF structures with the three torsional angles in *gauche* (see Table II).

The 13 low-energy conformations were confirmed by RHF/6-31G(d) and DFT calculations. They are: one FE (**Vb**), three OE (**Vi**, **Ve**, and **Va**), six OF (**Vf**, **Vk**, **Vc**, **Vj**, **Vh**, and **Vd**), and three FF

forms (**Vm**, **VI**, and **Vg**) (Fig. 7). Two FF conformations (**Vm** and **VI**) were annihilated at the DFT/IPCM level. Again, the global minimum varies as a function of the level of theory: **Va** at DFT/IPCM, **Vb** at RHF/6-31G(d) and DFT, **Vi** at MM2, and **Vf** at RHF/3-21G. It is clear, however, that the OE and FE forms are the preferred conformations at high levels of theory (Table III).

The RHF/3-21G, DFT, and DFT/IPCM results have been compared. Qualitatively, the three methods predict the same torsional potentials; however, DFT/IPCM calculations indicate higher energy barriers, making the conformational interconversion more restricted. On the basis of our results, RHF/3-21G calculations systematically underestimate the barrier to rotation. An estimation of the decisive role of the aqueous solvent on the conformational preferences of 3,4-dichloroimides was obtained by comparing the DFT/IPCM results with those obtained in vacuum. Although water introduces important changes in the relative energy ordering, the main effect of the solvent is to increase the relative energy range. Thus, in the gas phase the values range from 0.00–2.82 kcal/mol whereas in aqueous solution the conformational free energy ranges from 0.00–7.50 kcal/mol. Thus, the potential energy hypersurface $E = (\theta, \phi, \psi_1, \psi_2, \psi_3)$ is flatter in the gas phase than in the aqueous solution.

MOLECULAR ELECTROSTATIC POTENTIALS

Molecular recognition and the converse concept of specificity [34] are explained in mechanistic and reductionistic terms by a stereoelectronic complementarity between the binding molecule and the receptor [35]. In this context it is obvious that the knowledge of the stereoelectronic attributes and properties of 3,4-dichloromaleimides will contribute significantly to the elucidation of the mechanism of action at the molecular level. The intermolecular forces that contribute to both affinity and specificity can be schematically classified as hydrophobic and electrostatic ones. Thus, MEPs are of particular value because they permit visualization and assessment of the capacity of a molecule to interact electrostatically with a binding site. MEPs can be interpreted in terms of a stereoelectronic pharmacophore condensing all available information on the electrostatic forces underlying affinity and specificity.

Once the low-energy conformations for the different 3,4-dichloromaleimides were obtained and in an attempt to find the potentially reactive sites for

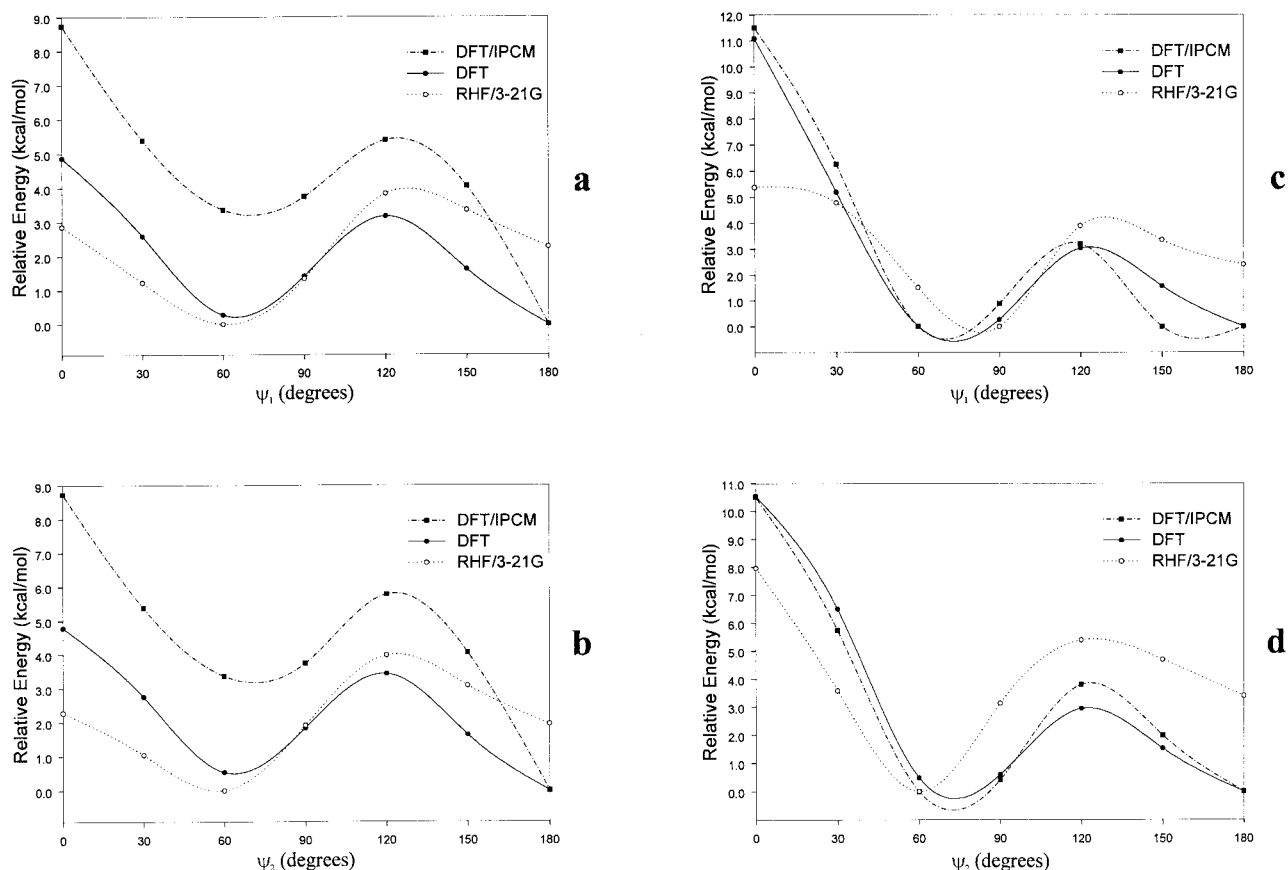


FIGURE 6. Comparison of PECs of torsional angles ψ_1 and ψ_2 obtained for compound **IV** in the fully extended conformation (**IVa**) (a and b). The same curves for the open folded conformation (**IVb**) are shown in (c) and (d); each PEC calculated at RHF/3-21G, DFT, and DFT/PCM levels of theory.

the ligands, we evaluated the electronic aspects of the molecules using MEPs. The electrostatic potential has long been applied as a guide to molecular reactive behavior [36–38]; for instance, the most negative values of MEP were interpreted as identifying and ranking sites for electrophilic attack, while its overall pattern served as the basis for qualitative analyses of biologic recognition interactions.

Figures 8 and 9 show the MEPs obtained for compounds **III**, **IV**, and **V**. These results account for the general characteristics of the electronic behavior of 3,4-dichloromaleimides reported here. The general pattern is similar for all of the systems. The MEPs exhibit two clear minimum values (deep red zones) in the vicinity of the 3,4-dichloroimido ring. This region is symmetrical with respect to the two carbonyl groups and displays a deep and extensive negative potential zone with values of about -40 (± 3) kcal/mol. In the benzene region a much smaller minimum was found [yellow areas with

$V(r) \cong -9$ (± 3) kcal/mol]. There are positive regions only near the carbonyl carbons [blue areas with $V(r) \cong +85$ (± 10) kcal/mol].

Compound **IV** in the FF conformation (**IVd**) changes the negative MEP region on the internal plane of the benzene ring to a neutral or positive region. Figures 9(a) and 9(b) illustrate this point well. The folded conformation of compound **III** (**IIIa**) displays a closely related behavior to that of **IVd** (results not shown). In contrast, the FF conformation of compound **V** (**Vg**) displays a MEP similar to those obtained for the extended conformations of compounds **III** and **IV** with negative potential at both sides of the benzene ring [Figs. 9(c) and 9(d)]. It is clear, however, that the FF structure of compound **IV** is more compact than and qualitatively not similar to the FF structure of compound **V**. The distance between the aromatic rings in the FF forms of compound **V** are substantially longer than those obtained for the **IIIa** and **IVd** conformations, respectively. MEPs of compounds **III–V** are confor-

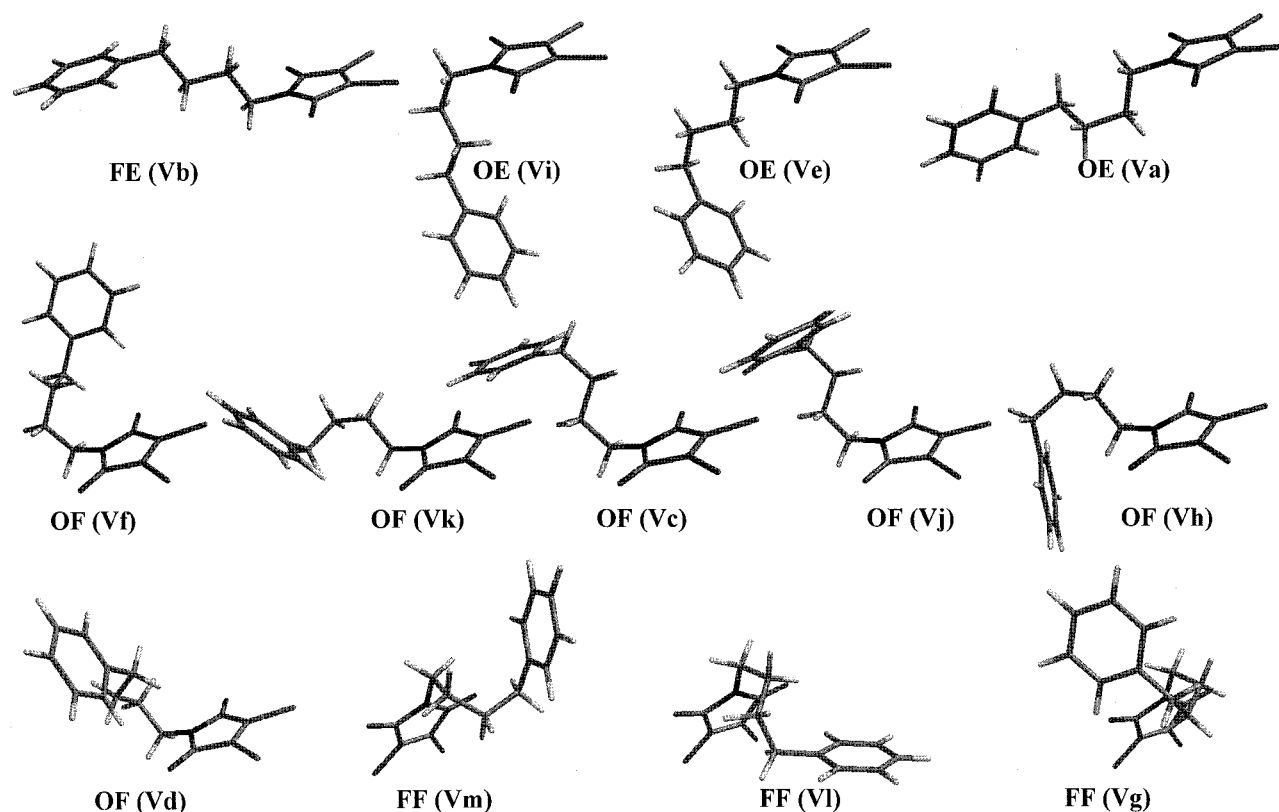


FIGURE 7. Spatial view of the 13 different conformations obtained for compound **V** (geometries were obtained from DFT calculations).

mationally dependent and as a result there may be a variation as a function of the spatial ordering of the aromatic rings. This result is not surprising: The MEP calculated from the electron density of a molecular system strongly depends on the relative spatial position of atoms, itself a function of the conformation of the molecule.

LOOKING FOR THE “BIOLOGICALLY RELEVANT CONFORMATION”

Using the simple notion of receptor-site occupancy one may seek chemical features common to 3,4-dichloromaleimides to suggest chemical binding sites. Thus, our results let us speculate that two binding sites would be necessary to produce the antifungal activity of these compounds. It may be imagined that the 3,4-dichloroimido ring engages the receptor at a specific site, without disregarding the fact that the rest of the molecule can contribute to additional binding by interacting with some accessory region. The molecular structure of these compounds appears to be critical for activity. The

fact that the activity is markedly affected when altering the length of the alkyl chain is suggestive of a cooperative effect between active groups, and it may be considered that the benzene group makes some kind of contribution to binding. The importance of chain length in the 3,4-dichloromaleimides raises the question of whether certain conformations may be associated with antifungal activity. If the antifungal activity of 3,4-dichloromaleimides requires two bonding sites, then it is possible to assume folded conformations of compounds **III** and **IV** may not be operative.

To determine the distances between the two potentially reactive centers (the two aromatic rings), the interatomic distances between N \cdots C \cdots (denoted in Table I) are compared. These distances are shown in the last column of Table III. Correlating the distances shown in Table III with antifungal activity (shown in Table I) it is reasonable to assume that the optimum interatomic distance between these groups to produce antifungal effect could be in the 3.5- to 5.0-Å range (marked in bold

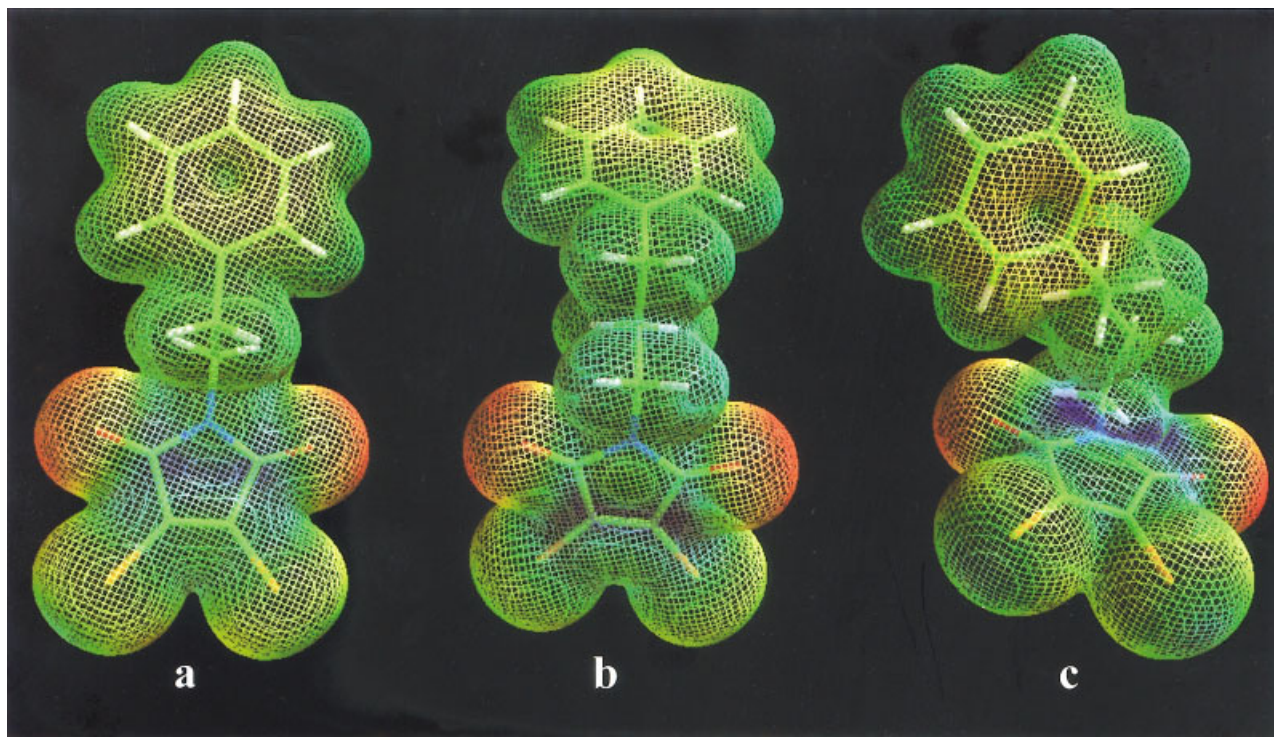


FIGURE 8. MEP energy isosurfaces of the **III**, **IV**, and **V** compounds are shown color-coded in the range from -43 (deepest red) to $+95$ kcal/mol (deepest blue). (a) Conformation **IIIb**; (b) conformation **IVa**; (c) conformation **Vd**.

in Table III). Thus, the lower activities obtained for compounds **I** and **II** might be explained in terms of their shorter distances with respect to the optimal one. The active compounds **III**, **IV**, and **V** are able to adopt this distance. However, it should be noted that only compound **IV**, the most active in this series, can adopt this spatial ordering without energy requirement. Compound **III** is too short and needs to be in an FE form (which is not the global minimum at the DFT/IPCM level of theory). These considerations may be applied to **V**, which is too large and needs to be in FF or OF conformation for favorably adopts an operative conformation. The preferred conformations for compound **V** are OE at the DFT/IPCM level and FE at the DFT level with distances of 6.0 and 6.4 Å, respectively. These distances exceed the optimal one and therefore it appears that a conformational rearrangement is necessary in compound **V** to adopt the biologically relevant conformation. Thus, in addition to the electronic effect, it is possible that conformational effects of the 3,4-dichloromaleimides also contribute to the activity of these compounds as antifungal agents.

MOLECULAR MODEL FOR THE BINDING MECHANISM OF 3,4-DICHLOROMALEIMIDES

Before a ligand can bind, there must be a relatively rigid complementary crevice inside the receptor that complements the ligand in shape to be able to accommodate it. Because complementarity is rarely perfect, more than one ligand can fit in the same crevice.

The process of conformational selection on binding the flexible 3,4-dichloromaleimides to a receptor can take different forms. Depending on the detailed mechanism of the binding process, the conformational characteristics of these compounds can assume varying degrees of importance. In principle, we can presume two general cases:

1. At any instant, only those 3,4-dichloromaleimides having the appropriate single conformation are able to bind to the receptor. Each portion of the maleimide molecule binds simultaneously to the appropriate subsite of the binding site. This model is associated with the idea that it is the preferred conformation in solution, which is the relevant one for bind-

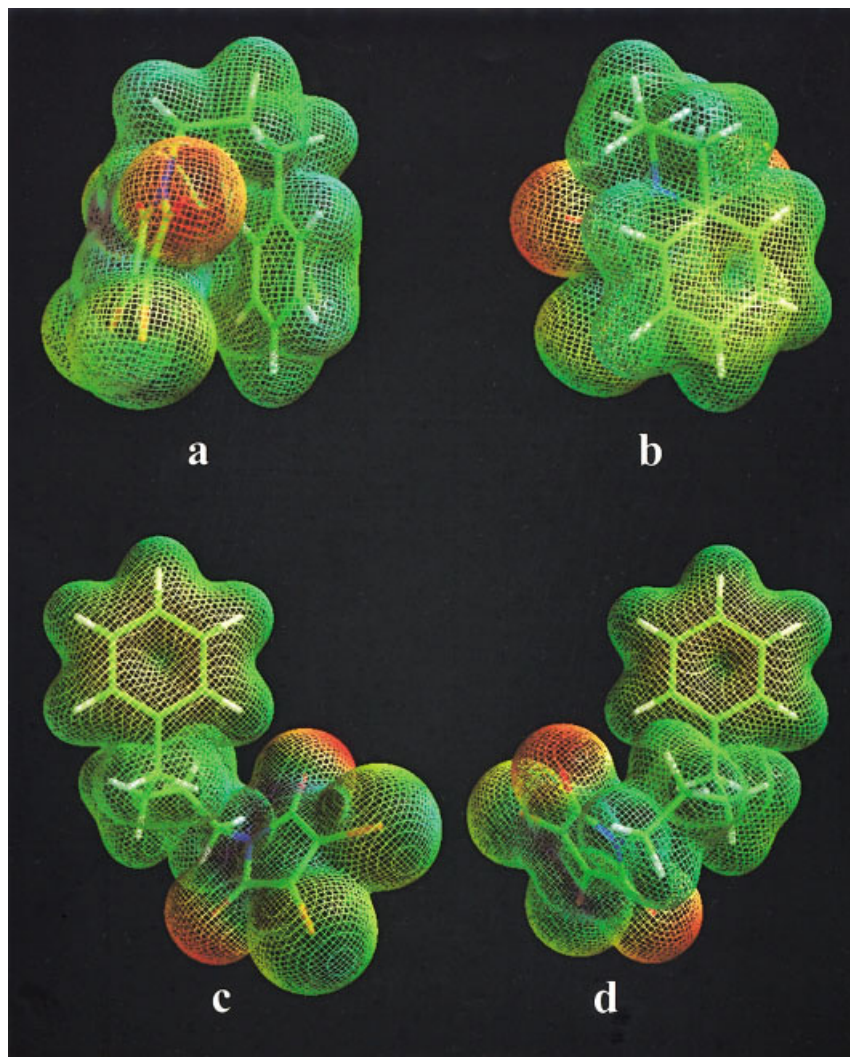


FIGURE 9. MEPs obtained for compounds **IV** and **V**. (a) Spatial view of the internal plane of benzene ring in conformation **IVd**; (b) spatial view of the external plane of benzene ring in conformation **IVd**; (c) spatial view of the internal plane of benzene ring in conformation **Vg**; (d) spatial view of the external plane of benzene ring in conformation **Vg**.

ing. However, in this case there is no a priori reason why this should be so. Also, there are a number of instances in which the conformation of a ligand bound to a protein has shown to be different from the preferred conformation in solution [39, 40].

2. Other possibility is that the binding takes place by a stepwise process in which an initial interaction between a single segment (the 3,4-dichloroimido ring) of maleimides in any conformation and its subsite is followed by a rapid rearrangement of the conformation of the 3,4-dichloromaleimide molecule so as to permit the binding of the remaining segment (the aryl group) to its subsite. An important

difference between this model and that of case 1 is that here the actual conformational distribution of 3,4-dichloromaleimides is less crucial, while the rate at which conformational interconversions can occur becomes considerably significant.

Accepting the validity of the DFT/IPCM method and of the obtained results, it seems that an intermediate model sharing aspects of both models (1 and 2) is in particular probable in the case of 3,4-dichloromaleimides. There is not a single and particular distance but a range of interatomic distances (from 3.5–5.0 Å) between the potentially reactive centers, which seem to be well tolerated to produce

the biologic response. However, it is clear that not any conformation is operative.

A high-energy barrier might force the molecule to bind by the "all-or-none" mechanism (model 1) rather than by the zipper mechanism (model 2). DFT/IPCM computations predict that barriers ranging from 3.5–11.5 kcal/mol are separating the different conformations and therefore the conformational interconversions are somewhat restricted but still available for these compounds. Also, a large part of the conformationally available space is accessible within a low value of energy with respect to the global minimum. This is an additional support for an intermediate model.

Conclusions

The presence of two symmetrical aromatic systems reduces notably the conformational possibilities of 3,4-dichloromaleimides. Thus, the conformational intricacies of these compounds, which in principle appear to be a complex problem, might be evaluated by relatively high levels of theory. In general, the different levels of theory reported here [MM2, RHF/3-21G, RHF/6-31G(*d*), and B3LYP/6-31G(*d*) (gas phase) and B3LYP/6-31++G(*d,p*)/6-31G(*d*) (aqueous phase)] displayed qualitatively comparable results indicating that molecular mechanic calculations and ab initio computations using a modest basis set like 3-21G are sufficient to realize exploratory conformational analysis. However, high levels of theory are necessary to confirm critical points and assign the conformational preferences. This is in particular apparent after examining that the global minimum obtained is different according to the employed levels of theory.

The inclusion of solvent effects appears to be at least prudent to consider the conformational interconversions. We used a continuum polarizable model (IPCM) to simulate the solvent effects. The simulations have some obvious limitations; nevertheless, a number of qualitative results are of interest. According to the results of ab initio and DFT calculations, it is clearly seen that the conformational preferences of molecule **III** change abruptly from vacuum to in solution. For the case of compound **IV**, the fully extended conformer **IVa** was found to be a global energy minimum both in vacuum [RHF/6-31G(*d*) and DFT methods] and in solvent (DFT/IPCM method). However, the profiles of the potential energy curves in solvent were different from those in vacuum. An obvious change in

the DFT/IPCM potentials was the energetic barriers at ψ_1 – ψ_3 torsionals, which increase with a dielectric constant of the medium, rendering the conformational space narrower in polar solvents than that in vacuum.

The conformational and electronic study including the use of MEPs allowed a model to be proposed for the recognition of the minimal structural requirements of the antifungal response by these 3,4-dichloromaleimides. Thus, the 3,4-dichloroimido ring and benzene group appear to be indispensable. Our results indicate that the optimum distance between these moieties is about 3.5–5.0 Å. A change of conformation of the small partner on attachment seems in particular probable in this case. Theoretical calculations including the solvent effects indicate that the active 3,4-dichloromaleimides display a moderate but still significant molecular flexibility, so adaptation of shape to reach the most favored binding positions is likely. Stepwise binding involving first the 3,4-dichloroimido ring followed by the rest of the molecule seems a reasonable possibility and there is some strongly suggestive evidence that this phenomenon take place.

ACKNOWLEDGMENTS

This work was supported by a grant from U.N.S.L. Some calculations were carried out on "Clementina" of Centro de Supercomputación, Buenos Aires, Argentina. The authors are indebted to a reviewer for suggestions. R.D.E. is a career researcher of CONICET—Argentina.

References

- Walsh, T. J. *Emerging Targets in Antibacterial and Antifungal Chemotherapy*; Chapman & Hall: New York, 1992; p. 349–373.
- White, T. C.; Marr, K. A.; Bowdenn, R. A. *Clin Microbiol Rev* 1998, 11, 382.
- Fromtling, R. A. *Drug New Prespect* 1999, 12, 557–569.
- Lopez, S. N.; Castelli, M. V.; Zacchino, S. A.; Dominguez, J. N.; Lobo, G.; Charris-Charris, J.; Cortés, C. G.; Ribas, J. C.; Devia, C. M.; Rodríguez, A. M.; Enriz, R. D. *Bioorg Med Chem* 2001, 9, 1999–2013.
- Urbina, J. M.; Cortés, C. G.; Palma, A.; López, S. N.; Zacchino, S. A.; Enriz, R. D.; Ribas, J. C.; Kouznetsov, V. *Bioorg Med Chem* 2000, 8, 691–698.
- Zacchino, S. A.; Yunes, R. A.; Filho, V. C.; Enriz, R. D.; Kouznetsov, V.; Ribas, J. C. In: Rai, M. K., ed. *The Need of New Antifungal Drugs. Screening for Antifungal Compounds with a Selective Mode of Action with Emphasis in*

- the Inhibitors of the Fungal Cell Wall. Haworth Press (in press).
7. Zacchino, S. A.; López, S. N.; Pezzenati, G.; Furlán, R. L.; Santecchia, C. B.; Muñoz, L.; Giannini, F. A.; Rodríguez, A. M.; Enriz, R. D. *J Nat Prod* 1999, 63, 1353–1357.
 8. Lopez, S. N.; Castelli, M. V.; Corrêa, R.; Filho, V. C.; Yunes, R. A.; Zamora, M. A.; Enriz, R. D.; Ribas, J. C.; Zacchino, S. A. *Bioorg Med Chem* (submitted for publication).
 9. (a) Becke, A. D. *Phys Rev A* 1998, 38, 3098–3100; (b) Becke, A. D. *J Chem Phys* 1993, 98, 5618–5652; (c) Lee, C.; Yang, W.; Parr, R. G. *Phys Rev B* 1998, 37, 785–789.
 10. Allinger, N. L. *J Am Chem Soc* 1977, 99, 8127–8134.
 11. Santágata, L. N.; Suvire, F. D.; Enriz, R. D.; Torday, L. L.; Csizmadia, I. G. *J Mol Struct Theochem* 1999, 465, 33–67.
 12. Santágata, L. N.; Suvire, F. D.; Enriz, R. D. *J Mol Struct Theochem* 2000, 507, 89–95.
 13. Santágata, L. N.; Suvire, F. D.; Enriz, R. D. *J Mol Struct Theochem* 2001, 536, 173–188.
 14. Santágata, L. N.; Suvire, F. D.; Enriz, R. D. *J Mol Struct Theochem* 2001, 571, 91–98.
 15. Foresman, J. B.; Keith, T. A.; Wiberg, K. B.; Snoonian, J. *J Phys Chem* 1996, 100, 16098–16104.
 16. Miertus, S.; Scrocco, E.; Tomasi, J. *Chem Phys* 1981, 55, 117–129.
 17. Radkiewicz, J. L.; Clarke, S.; Zipse, H.; Houk, K. N. *J Am Chem Soc* 1996, 118, 9148–9155.
 18. Jhon, J. S.; Kang, Y. K. *J Phys Chem A* 1999, 103, 5436–5439.
 19. Shukla, M. K.; Mishra, S. K.; Kumar, A.; Mishra, P. C. *J Comput Chem* 2000, 21, 826–846.
 20. Bandyopadhyay, P.; Gordon, M. S. *J Chem Phys* 2000, 113, 1104.
 21. Frisch, M. J.; Trucks, G. W.; Schlegel, H. B.; Scuseria, G. E.; Robb, M. A.; Cheeseman, J. R.; Zakrzewski, V. G.; Montgomery, J. A. Jr.; Stratmann, R. E.; Burant, J. C.; Dapprich, S.; Millam, J. M.; Daniels, A. D.; Kudin, K. N.; Strain, M. C.; Farkas, O.; Tomasi, J.; Barone, V.; Cossi, M.; Cammi, R.; Mennucci, B.; Pomelli, C.; Adamo, C.; Clifford, S.; Ochterski, J.; Petersson, G. A.; Ayala, P. Y.; Cui, Q.; Morokuma, K.; Malick, D. K.; Rabuck, A. D.; Raghavachari, K.; Foresman, J. B.; Cioslowski, J.; Ortiz, J. V.; Baboul, A. G.; Stefanov, B. B.; Liu, G.; Liashenko, A.; Piskorz, P.; Komaromi, I.; Gomperts, R.; Martin, R. L.; Fox, D. J.; Keith, T.; Al-Laham, M. A.; Peng, C. Y.; Nanayakkara, A.; Gonzalez, C.; Challacombe, M.; Gill, P. M. W.; Johnson, B.; Chen, W.; Wong, M. W.; Andres, J. L.; Gonzalez, C.; Head-Gordon, M.; Replogle, E. S.; Pople, J. A. *Gaussian 98, Revision A.7*; Gaussian, Inc.: Pittsburgh, PA, 1998.
 22. Politzer, P.; Truhlar, D. G. *Chemical Applications of Atomic and Molecular Electrostatic Potentials*; Plenum Publishing: New York, 1991.
 23. Carrupt, P. A.; El Tayar, N.; Karlé, A.; Festa, B. *Meth Enzymol* 1991, 202, 638–677.
 24. Greeling, P.; Langenaeker, W.; De Proft, F.; Baeten, A. *Molecular Electrostatic Potentials: Concepts and Applications. Theoretical and Computational Chemistry, Vol. 3*; Elsevier Science B. V.: Amsterdam, 1996; p. 587–617.
 25. Jáuregui, E. A.; Ciuffo, G. M.; Enriz, R. D. *Temas Actuales de Química Cuántica, Vol. 29*; UAM Ediciones, Barcelona 1997; p. 327–349.
 26. PC SPARTAN PRO; Wavefunction, Inc.: Pittsburgh, PA, 1996–2000.
 27. Feigel, M. *J Mol Struct Theochem* 1966, 366, 83–88.
 28. Villagra, S. E.; Santillan, M. B.; Rodríguez, A. M.; Chasse, G. A.; Freile, M. L.; Zacchino, S. A.; Matyus, P.; Enriz, R. D. *J Mol Struct Theochem* 2001, 549, 217–228.
 29. Rodríguez, C. F.; Vuckovic, D. L.; Hopkinson, A.-C. *J Mol Struct Theochem* 1996, 363, 131–136.
 30. Farkas, Ö.; Salpietro, S. J.; Csizmadia, I. G. *J Mol Struct Theochem* 1996, 367, 25–31.
 31. Csizmadia, I. G. *The Chemistry of the Thiol Group*; John Wiley & Sons: New York, 1974; chapter 1.
 32. Peterson, M. R.; Csizmadia, I. G. *J Am Chem Soc* 1978, 100, 6911–6916.
 33. Peterson, M. R.; Csizmadia, I. G. *Progress of Theoretical Organic Chemistry, Vol. 3*; Elsevier: Amsterdam, 1982; p. 190–266.
 34. Sarai, A. *J Theor Biol* 1989, 140, 137.
 35. North, A. C. T. *J Mol Graph* 1989, 7, 67.
 36. Scrocco, E.; Tomasi, J. *Topics Curr Chem* 1973, 42, 95.
 37. Politzer, P.; Murray, J. S. In: Lipkowitz, K. B.; Boyd, D. B., eds. *Reviews in Computational Chemistry, Vol. 2*; VCM: New York, 1991; chapter 7.
 38. Naray-Szabo, G.; Ferenczy, G. G. *Chem Rev* 1995, 95, 829.
 39. Meadows, D. H.; Roberts, G. C. K.; Jardetzky, O. *J Mol Biol* 1969, 45, 491.
 40. Rogerds, P.; Roberts, G. C. K. *FEBS Lett* 1973, 36, 330–333.